Publication III

Pia Myllymäki, Martin Roeckerath, Joao Marcelo Lopes, Jürgen Schubert, Kenichiro Mizohata, Matti Putkonen, and Lauri Niinistö. 2010. Rare earth scandate thin films by atomic layer deposition: effect of the rare earth cation size. Journal of Materials Chemistry, volume 20, number 20, pages 4207-4212.

Rare earth scandate thin films by atomic layer deposition: effect of the rare earth cation size

Pia Myllymäki,*[a] Martin Roeckerath,[b] Joao Marcelo Lopes,[b] Jürgen Schubert,[b] Kenichiro Mizohata,[c] Matti Putkonen[ad] and Lauri Niinistö[a]

Received 9th February 2010, Accepted 24th March 2010
First published as an Advance Article on the web 14th April 2010
DOI: 10.1039/c0jm00363h

A series of amorphous $REScO_3$ films was deposited by atomic layer deposition (ALD) using rare earth (RE) β-diketonate precursors $RE(thd)_3$ (thd = 2,2,6,6-tetramethyl-3,5-heptanedionato) together with ozone in an attempt to study the effect of the RE^{3+} cation size on various film properties. A clear correlation between the deposition rate and the RE^{3+} cation radius was established. $REScO_3$ films with a metal ratio RE : Sc close to the stoichiometric one, *viz.* RE : Sc = 1, and a small excess of oxygen were realized by adjusting the metal precursor pulsing ratio. Small amount of carbon was found as impurity in all the films, concentrations varying from 1–3 at% (RE = La, Gd or Dy) to 0.4–0.5 at% (RE = Er or Lu). Also the crystallization temperature and the resulting phase were affected by the RE^{3+} cation size. The $REScO_3$ films were found to crystallize either as an orthorhombic perovskite phase or as a solid solution of the cubic C-type oxides. High crystallization temperatures of 800–900 °C were observed for $LaScO_3$, $GdScO_3$ and $DyScO_3$. All the films gave smooth *C–V* curves with very small hysteresis (typically <35 mV). The highest dielectric constant ($\kappa \approx 24$) was found for DyScO3. Also the leakage current densities were small, typically in a range of 10^{-6}–10^{-9} A cm^{-2} at 1 V. The results confirm that $REScO_3$ films deposited by ALD are potential candidates for new generation high-κ gate dielectrics.

Introduction

Continued downscaling of metal-oxide-semiconductor field-effect transistors (MOSFETs) has led to a search for new materials to replace SiO_2 as gate insulator. Until recently, the Si–SiO_2 system has been an ideal system from electrical, material and processing point of view. This presents many challenges for the new candidates. In addition to the electrical properties (high dielectric constant, large band gap and offset to silicon, low leakage current) new candidates must fulfill many material and processing requirements, including high interface quality, low density of interface and bulk states, chemical stability with respect to both silicon and the metal gate, as well as compatibility with the CMOS process.[1] Either amorphous or high quality single crystal structure is required to minimize the leakage current or diffusion paths.

Due to their many desirable properties (*e.g.* high dielectric constant, high crystallization temperature, large band gap and offset to silicon), rare earth scandate ($REScO_3$) thin films have gained considerable interest as possible high-κ dielectric materials.[2,3] Especially $GdScO_3$[4,5] and $DyScO_3$[6–8] have been widely studied. New studies frequently appear, some of the most recent candidates being $SmScO_3$[9] and $TbScO_3$.[10]

The rare earth elements (*i.e.* lanthanoids Ln, yttrium and scandium) form a very interesting group of elements with many similar properties. Due to the gradual reduction in the cation size within the lanthanoid series, *i.e.* the lanthanoid contraction, many properties also periodically change within the group. Binary RE sesquioxides RE_2O_3 can adopt different structures depending on the temperature and the RE^{3+} cation size, the hexagonal A-type and the cubic C-type being the most common at low and moderately elevated temperatures.[11] Larger RE elements prefer the A-form, whereas the smaller RE elements prefer the cubic C-type similar to the cubic bixbyite structure. Yttrium being similar in size with erbium and holmium, and scandium being clearly the smallest of the group, they both prefer the C-type structure. Depending on the size difference between Sc and the other RE in structure, ternary $REScO_3$ films can adopt either an orthorhombic perovskite structure or form a solid solution having the cubic C-type structure. In the bulk form, ternary $REScO_3$ phases with the perovskite structure have been synthesized at ambient pressure when RE = La, Pr, Nd, Sm, Eu, Gd, Tb, Dy and Ho.[12] Heavier lanthanoids (Er–Lu) and Y do not form perovskites under ambient conditions, but high-pressure syntheses of $YScO_3$, $HoScO_3$, $ErScO_3$ and $TmScO_3$ have been reported.[13]

Compared to bulk form, materials may behave very differently as thin films, where the deposition method as well as the substrate has an effect on many of the thin film properties. Low-energy interfaces can facilitate the formation of otherwise unstable compounds or structures. Crystallization behavior of $REScO_3$ thin films deposited by pulsed laser deposition (PLD) on $LaAlO_3$ substrates has been recently studied and a correlation between the atomic number and the crystallization temperature has been

[a]*Laboratory of Inorganic Chemistry, Department of Chemistry, Aalto University School of Science and Technology, FI-00076 Aalto, Finland. E-mail: pia.myllymaki@tkk.fi*
[b]*Institute of Bio and Nanosystems, JARA-Fundamentals of Future Information Technologies, Research Centre Jülich, D-52425 Jülich, Germany*
[c]*Division of Materials Physics, Department of Physics, University of Helsinki, FI-00014, Finland*
[d]*Beneq Oy, P.O. Box 262, FI-01511 Vantaa, Finland*

found.[14] $REScO_3$ perovskite phase was detected when RE = La–Ho, but $TmScO_3$, $YbScO_3$ and $LuScO_3$ did not form the perovskite phase in the temperature range studied (800 °C and below). With a suitable substrate material, even the smallest of the lanthanoid series, *viz.* Lu has been reported to form a perovskite phase when deposited onto $NdGaO_3$(110) and $DyScO_3$(110) substrates.[15]

In this paper, we have attempted to explore how the reduction in the cation size affects some properties of the ALD-deposited rare earth scandate thin films. To investigate this, we have chosen to study the $LaScO_3$, $DyScO_3$, $ErScO_3$ and $LuScO_3$ thin films. This series includes the largest (La) and the smallest (Lu) element in the group. Especially the region, where the change in crystal structure from perovskite to solid solution is to be expected, was investigated in more detail. Moreover, results from previously published processes of $YScO_3$[16] and $GdScO_3$[5] thin films were included for comparison. β-Diketonate type $RE(thd)_3$ (thd = 2,2,6,6-tetramethyl-3,5-heptanedionato) metal precursors were used for two main reasons. Firstly, they can easily be synthesized for all the RE elements covered in this study and besides ALD processes of these rare earth oxides have been well documented using thd-precursors.[17] Secondly, by using these precursors the depositions could be carried out at the same temperature (300 °C). Furthermore, we have earlier demonstrated in our study of $YScO_3$ films that some properties, *e.g.* crystallization behavior and electrical properties, are affected by the choice of precursors,[16] which is another reason to use the same type of metal precursors for all the depositions.

Experimental

Film deposition

$REScO_3$ thin films were deposited in a hot-wall flow-type ALD F-120 reactor manufactured by ASM Microchemistry. $RE(thd)_3$ precursors were synthesized by the method described by Eisentraut and Sievers[18] and subsequently purified by sublimation. In the ALD reactor, metal precursors were sublimed from open glass crucibles at the sublimation temperatures listed in Table 1. Sublimation temperature for $Sc(thd)_3$ was 115–118 °C. Metal precursor pulse and purge lengths were 1.0 s and 1.5 s, respectively. Ozone produced from 99.999% O_2 in Fischer Model 502 ozone generator was used as the oxygen source. Ozone pulse and purge lengths were 1.5 s and 2.0 s, respectively. Nitrogen (99.999+%) was used as both the carrier and purge gas and was obtained from air using a Nitrox UHPN 3000-1 nitrogen generator. The deposition temperature was 300 °C and the pressure in the reactor during the depositions was 2–3 mbar. Films were deposited onto two 5 × 5 cm p-type Si(100) substrates (Okmetic Ltd, Vantaa, Finland). Glass substrates of similar size were used on the backside to prevent film growth on the back of silicon. Silicon substrates were mostly used as received, but substrates for the samples intended for electrical characterization were dipped prior to the depositions into 2% HF solution to remove the native oxide layer.

Table 1 Metal precursor sublimation temperatures, pulsing ratios for films with composition close to the stoichiometric value, and the resulting growth rates for the $REScO_3$ films

$RE(thd)_3$	$RE(thd)_3$ sublimation temperature/°C	RE : Sc pulsing ratio	Growth rate (thickness 5–20 nm)/Å per cycle	Growth rate (thickness > 50 nm)/Å per cycle
$La(thd)_3$	165–170	5 : 6	0.28	0.26
$Gd(thd)_3$	138	5 : 6	0.21	0.21
$Dy(thd)_3$	125–128	10 : 11	0.18	0.19
$Er(thd)_3$	130	1 : 1	0.19	0.19
$Lu(thd)_3$	125	6 : 5	0.18	0.18

The metal precursor pulsing ratio RE : Sc and the number of deposition cycles were varied to afford films with the desired composition and thickness, respectively. During the optimization of the deposition parameters, the metal ratio RE : Sc was measured by X-ray fluorescence (XRF, Philips PW 1480 WDS spectrometer) using Rh excitation. The data were analyzed with the UniQuant 4.34 program (Omega Data Systems, Netherlands), which is based on fundamental parameters and experimentally determined instrumental sensitivity factors.[19,20] When a metal ratio close to the stoichiometric one, *viz.* RE : Sc = 1, was observed, samples of different thicknesses from 5 nm to *ca.* 100 nm were deposited. The growth rates for films with thickness >50 nm were calculated from thickness data determined by an optical fitting method described by Ylilammi and Ranta-aho.[21] In this method, theoretical spectra were fitted to reflectance spectra (190–1100 nm) measured in a Hitachi U-2000 double beam spectrophotometer. The film thickness for thinner films (from 5 nm to 20 nm) was determined by XRR at an angle of incidence of 1° to 5°. Optimized precursor pulsing ratios and deposition rates for the nearly stoichiometric films are presented in Table 1.

Characterization

The RE : Sc metal ratio was determined by Rutherford backscattering spectrometry (RBS) with He^+ ions at an energy of 1.4 MeV. The amount of light elements and the metal to oxygen ratio M : O were determined by time-of-flight elastic recoil detection analysis (TOF-ERDA)[22] at the Acceleration Laboratory of the University of Helsinki. A beam of $^{79}Br^{9+}$ ions at 48 MeV was obtained from a 5 MV tandem accelerator EGP-10-II. The speciation of carbon impurities was investigated by Fourier transform infrared (FT-IR) spectroscopy in a Nicolet Magna-750 infrared spectrometer. Selected samples were analyzed before and after thermal annealing. The crystal structure of the films was determined before and after thermal annealing by X-ray diffraction (XRD) using Cu K_α radiation (Philips MPD 1880). Selected samples were also analyzed by GIXRD (Panalytical X'Pert Pro MDP diffractometer). Thermal annealings for 10 min were carried out in a PEA 601 (ATV Technologie GmbH) rapid thermal annealing oven under flowing nitrogen. Annealing temperatures varied between 500 °C and 1000 °C.

For the electrical characterization, capacitor stacks were prepared. The top contacts were realized by depositing platinum using electron beam evaporation through a shadow mask. The pads were 65 by 65 μm^2 large and approximately 70 nm thick. The deposition was performed at a pressure of 3–6 × 10^{-6} mbar with a deposition rate of 1.3 Å s^{-1}. Prior to the deposition, the samples were heated to 200 °C and kept there for 10 min in order to remove the adsorbed water. For the backside contact, 200 nm of Al were deposited under the same pressure and with a rate of 8 Å s^{-1}. A forming gas annealing (90% N_2/10% H_2) was

performed at 400 °C for 10 min to reduce interface states between the high-κ film and the silicon substrate and to improve the backside contact. The electrical characterization of the capacitor stacks was performed on a measuring stage with precisely movable measuring tips. *C–V* curves were recorded with an impedance analyzer (HP 4192A) at a frequency of 100 kHz and a hold time of 3 s per point. *I–V* curves were recorded with a semiconductor parameter analyzer (HP 4155B) using a hold time of 30 s at each measuring point.

Table 2 Film compositions according to RBS and TOF-ERDA

$REScO_3$	Pulsing ratio RE : Sc	Measured RE : Sc	M : O ratio	C (at%)	H/at%	F/at%
$LaScO_3$	5 : 6	0.97	0.57	2.7 ± 0.2	1.8 ± 0.1	2.0 ± 0.2
$GdScO_3$	10 : 11	1.02	0.65	0.9 ± 0.1	1.9 ± 0.1	2.9 ± 0.2
$DyScO_3$	5 : 6	1.06	0.66	1.3 ± 0.3	2.3 ± 0.2	0.7 ± 0.2
$ErScO_3$	1 : 1	1.17	0.55	0.5 ± 0.1	1.3 ± 0.2	3.8 ± 0.5
$LuScO_3$	6 : 5	1.22	0.64	0.4 ± 0.1	1.5 ± 0.1	2.8 ± 0.3

Results and discussion

Film deposition

Table 1 summarizes the $REScO_3$ thin film growth rates and metal precursor pulsing ratios used to achieve the stoichiometric metal ratio RE : Sc ≈ 1. As expected, the growth rates of the $REScO_3$ thin films increase as the RE^{3+} cation radius increases. The same trend has been reported for the binary RE_2O_3 thin films.[17] The film thickness was linearly dependent on the number of the deposition cycles and the growth rates for the thicker and the thinner films were same within experimental error which is typical for an ALD process.[23]

Film composition

According to RBS, all films had a metal ratio close to the stoichiometric one, *viz.* RE : Sc = 1, in particular for lighter REs, as can be seen in Table 2. Based on preliminary XRF results, a small excess of Sc was needed to deposit stoichiometric films except for $ErScO_3$ and $LuScO_3$. In these cases, it was sufficient that an equal amount of RE and Sc or even a slight excess of RE was pulsed into the film which resulted in slightly RE rich films. Table 2 also presents the metal to oxygen ratio and concentration of light elements in the films as determined by TOF-ERDA.

Carbon is a common impurity in ALD-deposited thin films when carbon-containing precursors are used. As can be seen in Table 2, films with larger REs have more carbon (~3 to 1 at%) than films with smaller REs (≤0.5 at%). It has been reported earlier that La_2O_3 films deposited by ALD using the same thd-precursor as here together with ozone contain relatively high amounts of carbon[24] (8–10 at% at the deposition temperature range 300–325 °C). Incorporation of another metal into the La_2O_3 film considerably reduces the presence of carbon. A similar ALD process as here to deposit $LaAlO_3$ thin films using β-diketonate precursors resulted in films with 2.4 at% of carbon at the deposition temperature of 325 °C and only 0.8 at% at the deposition temperature of 400 °C.[25] Binary oxide films of smaller REs, *viz.* Y_2O_3[26] and Sc_2O_3,[27] contained only a very small or negligible amount of carbon (1.0–1.4 at% or <0.1 at% at the deposition temperature 350 °C, respectively). The amount of carbon found here is in good accordance with these earlier findings. There is also some hydrogen and fluorine in the films. The level of hydrogen (1–2 at%) found in the films is approximately the same as was found previously in binary RE_2O_3 films deposited by the thd-process.[17] A small fluorine impurity is common when ozone is used in our reactor and assumed to originate from the vacuum grease or the Teflon gaskets used in the reactor. Therefore it could probably be eliminated by different reactor design and choice of materials.

The type of carbon impurities was studied in more detail by FT-IR spectroscopy. A typical doublet at ~1500 to 1400 cm^{-1} (shown in Fig. 1a) and a singlet at ~850 cm^{-1}, resulting from the unidentate carbonate group,[28] could be identified especially in the case of larger REs. This is to be expected when a strong

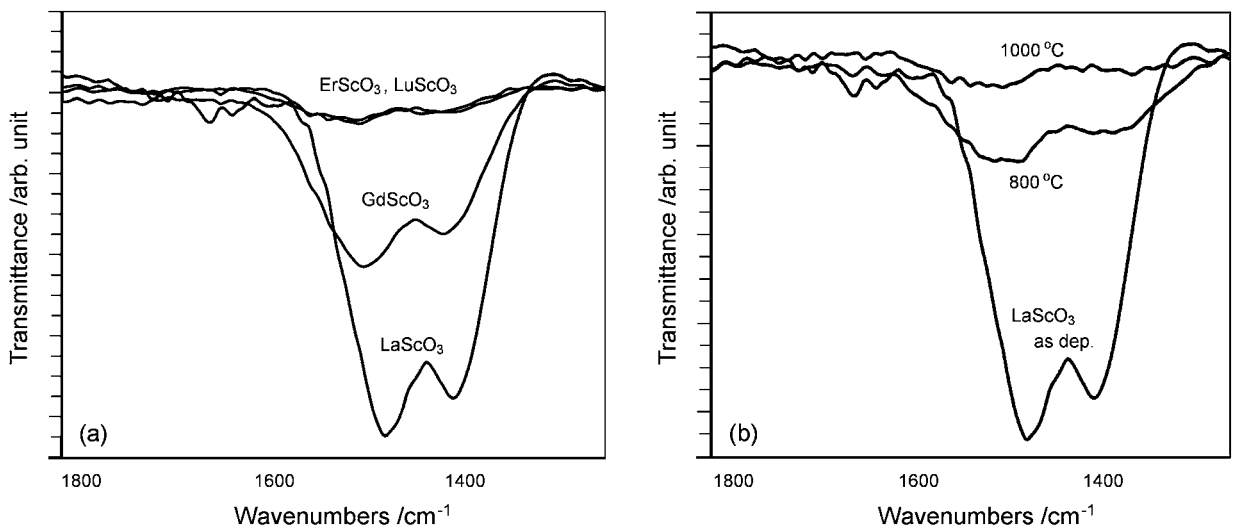

Fig. 1 (a) FT-IR spectra of as-deposited $LaScO_3$, $GdScO_3$, $ErScO_3$ and $LuScO_3$ films showing typical doublet band of carbonate group. (b) The effect of annealing on amount of carbonate in $LaScO_3$ films as shown by the decrease of the doublet intensity.

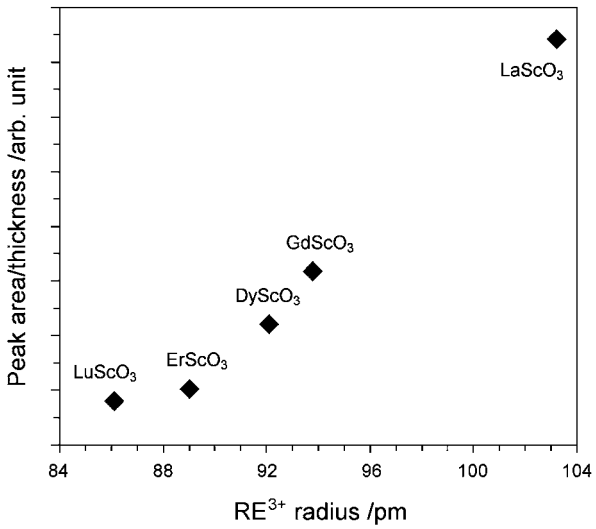

Fig. 2 Normalized carbonate doublet peak areas *versus* RE^{3+} cation radius indicating a clear trend in the amount of carbonate found in $REScO_3$ films.

oxidizer such as ozone is used together with a precursor containing carbon. Also the diminishing of the carbonate doublet can be seen in Fig. 1a as the RE cation becomes smaller. In order to investigate the effect of thermal treatment on the amount of carbonate, the $LaScO_3$ films were analyzed also after the thermal treatment. Annealing at 800 °C clearly reduced the intensity of the doublet, and after annealing at 1000 °C the doublet band was barely noticeable (Fig. 1b). In Fig. 2 the normalized peak area is depicted as a function of the RE^{3+} cation radius, showing a clear correlation between the amount of carbonate and the cation size.

According to TOF-ERDA, all the films contained some excess oxygen. This can be partly explained by the presence of carbonate (especially in the case of $LaScO_3$), but for the $ErScO_3$ film, where the carbon content is very small, there still is a considerable amount of excess oxygen. One explanation for the observed high oxygen content in all the films could be the fact that the interfacial SiO_2 layer is very difficult to distinguish by TOF-ERDA and, therefore, the actual amount of oxygen in the $REScO_3$ film could well be slightly lower than that detected by TOF-ERDA. However, this does not explain why the amount of oxygen in $ErScO_3$ film is so much higher than expected. Another possible explanation could be the fact that the $ErScO_3$ sample analyzed by TOF-ERDA was deposited onto a silicon substrate from a different batch, which may have been of lower quality having a thicker native SiO_2 layer at the surface. A more detailed analysis is obviously needed to fully explain this phenomenon.

Crystallization behavior

An amorphous structure is ideal for a gate dielectric film, since there are no dislocations nor grain boundaries that can act as possible pathways for leakage current or diffusion. During the CMOS manufacturing process high temperatures are used and therefore high crystallization temperature is important for the gate insulator material to stay amorphous.

According to the XRD data, all the $REScO_3$ thin films were amorphous after the deposition except for $LuScO_3$, which showed weak diffraction peaks of the cubic C-type structure even before the thermal annealing. After thermal annealing, all films eventually started to crystallize and form polycrystalline structures. First signs of crystallinity were detected at 600 °C ($ErScO_3$), 800 °C ($LaScO_3$) and 900 °C ($DyScO_3$). According to our earlier studies, $YScO_3$ and $GdScO_3$ start to crystallize at 1000 °C[16] and 900 °C,[5] respectively. Diffraction patterns of annealed $LaScO_3$, $DyScO_3$ and $LuScO_3$ measured at a grazing incidence mode are shown in Fig. 3. Larger REs (La–Gd) formed the orthorhombic perovskite phase as expected while smaller ones preferred the cubic C-type solid solution. $DyScO_3$ showed an interesting behavior: after annealing at 900 °C only peaks of the C-type solid solution were clearly visible but after annealing at 1000 °C also peaks of the perovskite phase became visible from the background. In earlier studies, $DyScO_3$ films are reported to crystallize as hexagonal Dy_2O_3[2,4,7] or as perovskite phase $DyScO_3$,[8] depending mainly on the substrate material. A bulk study on high pressure synthesis of $DyScO_3$ revealed that both C-type solid solution and perovskite phase had formed, but after prolonged annealing at high pressure only the perovskite phase was detected.[13] However, some recent publications have given new information concerning the behavior of the silicon/$REScO_3$ interface.[29–31] It has been shown that MOCVD-deposited $DyScO_3$ films react with the underlying SiO_2 layer at temperatures ~800 °C and thereupon an amorphous silicate layer is formed.[29,30] The same phenomenon was also detected with $LaScO_3$ films deposited by molecular beam deposition (MBD).[31] The extent of Si diffusion seems to depend on many factors, *e.g.* annealing temperature, atmosphere and the quality of the SiO_2 layer between the silicon substrate and the $REScO_3$ film. Also the thickness of the original $REScO_3$ layer plays a significant role. At

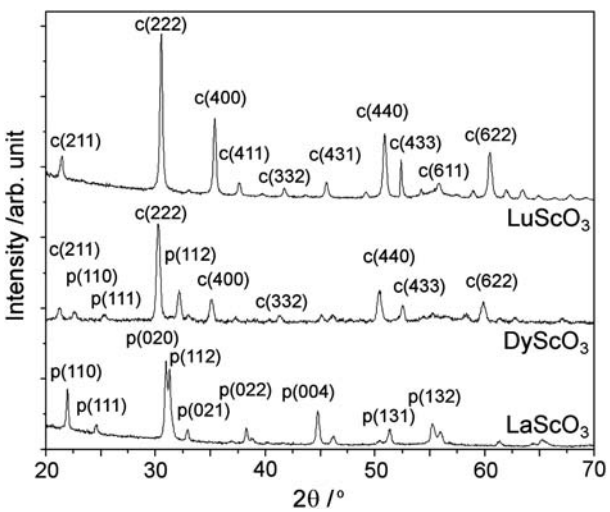

Fig. 3 GIXRD patterns of $LaScO_3$ (after annealing at 800 °C), $DyScO_3$ (1000 °C) and $LuScO_3$ (600 °C). $LaScO_3$ crystal structure can be identified as orthorhombic perovskite type (ICDD reference code 01-074-4348) and $LuScO_3$ as cubic C-type (reference code 04-002-0541). Most intense peaks of both phases (labeled "c" for cubic C-type and "p" for perovskite) can be identified in diffraction patters of $DyScO_3$ (reference code 00-027-0204 for perovskite).

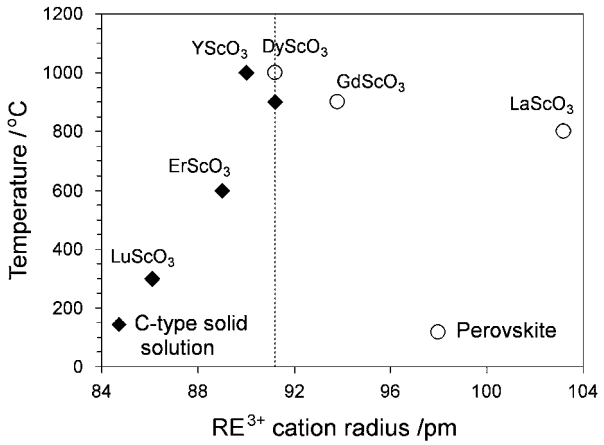

Fig. 4 $REScO_3$ crystallization temperatures and phases detected *versus* the RE^{3+} cation radius.

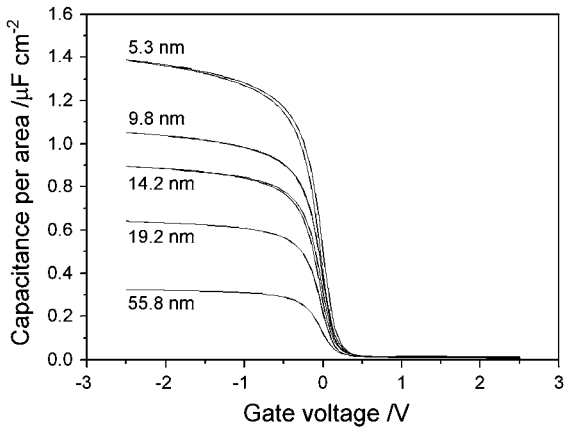

Fig. 5 *C–V* curves of $DyScO_3$ films with varying thicknesses.

1000 °C, a thin (~4 nm) $DyScO_3$ film was completely transformed into amorphous $Dy_xSc_ySi_zO_\delta$ layer,[29] but in the case of an originally thicker (~12 nm) $DyScO_3$ film, a polycrystalline $DyScO_3$ layer was formed on top of an amorphous silicon rich layer.[30] The size of the crystals was very small, which explains why they were not detected by X-ray diffraction methods. Due to the similarities within the lanthanoid group, it is likely that other $REScO_3$ films behave similarly as well. When the reaction between binary RE_2O_3 films and silicon substrates was investigated after thermal annealing, it was concluded that the larger the ionic radius of the RE^{3+} is, the more easily Si diffuses into the RE_2O_3 film.[32] In the scope of this paper, however, we did not investigate the possible reactions between the $REScO_3$ films and the substrate in more detail, but it is quite possible that similar reactions occur also with ALD-deposited $REScO_3$ films.

Fig. 4 summarizes the crystallization behavior of the $REScO_3$ films studied. Crystallization temperatures are relatively high for the perovskite films obtained close to the phase transition zone (800–1000 °C), but they decrease rapidly when the RE^{3+} cation size becomes smaller and the cubic solid solution becomes more favorable.

Electrical properties

$REScO_3$ films with thicknesses varying from 5 to 20 nm (and also 55 nm for $DyScO_3$) were subjected to electrical characterization. *C–V* curves were smooth without any humps or irregularities and almost free of hysteresis (typically <35 mV) indicating a low density of oxide charges in the films. Only in the case of the thinnest (5 nm and 10 nm) $LaScO_3$ films the hysteresis was slightly larger, *viz.* in the range of 55–90 mV. Flat band voltages were typically between 0.05 V and 0.2 V, except for $ErScO_3$ where a larger variation from −0.03 mV to 0.4 mV was observed. *C–V* curves for $DyScO_3$ are shown in Fig. 5.

CETs (capacitance equivalent thicknesses) calculated from capacitances taken at a gate voltage of −2 V were plotted *versus* the physical film thicknesses resulting in straight lines where the dielectric constants could be extracted from the slopes. The highest dielectric constant was found for $DyScO_3$ (~24), which is slightly higher than values found in films deposited with PLD[2] or MOCVD[7] (~22). For $LaScO_3$, κ values from 16 to 22 have been reported earlier,[2,3,31] and in this case $\kappa \approx 16$ was extracted from the CET plot. The dielectric constant for $LuScO_3$ deviates most from the rest of the series being only ~11, which is close to what has been reported for binary RE_2O_3 oxides.[17]

Table 3 Summary of the electrical properties of $REScO_3$ films. The results on $GdScO_3$ thin films published earlier[5] are also included for comparison

$REScO_3$	κ	Leakage current density at 1 V (5 nm film)/A cm^{-2}	Flat band voltage/V	Hysteresis/mV
$LaScO_3$	16.2	$\sim10^{-6}$	0.05–0.2	50–90 (5–10 nm) 10–30 (15–20 nm)
$GdScO_3$	22	$\sim10^{-7}$ to 10^{-8}	0.02–0.13	~100 (5 nm) < 100 (10–20 nm)
$DyScO_3$	24	$\sim10^{-7}$ to 10^{-8}	0.13–0.23	20–25 (5–15 nm) < 10 (20–55 nm)
$ErScO_3$	17.6	$\sim10^{-4}$	−0.03 to 0.4	5–30 (5–20 nm)
$LuScO_3$	10.9	$\sim10^{-9}$	0.04–0.12	15–24 (5–10 nm) < 5 (15–20 nm)

Leakage current densities for all films (Table 3) were small. Again results for $LuScO_3$ were somewhat surprising. Although, as revealed by XRD, $LuScO_3$ films (~80 to 100 nm) had partly crystallized during the deposition, which in many cases leads to higher leakage current densities, the measured leakage current density of 5 nm $LuScO_3$ film was still the lowest in the series. However, it is possible that the very thin sample analyzed for leakage current may have been amorphous, if the crystallization during the deposition only takes place when the film thickness reaches a certain critical value.

Conclusions

Ternary $REScO_3$ thin films were deposited by ALD using β-diketonate type precursors and ozone. At 300 °C the film growth rate increased as the RE^{3+} cation radius increased. Also the amount of carbon impurities found in the films by TOF-ERDA and FT-IR spectroscopy increased with the increasing RE^{3+} cation radius and the basicity of the cation.

The crystallization behavior of the $REScO_3$ films was studied after thermal annealings by XRD and, depending on the RE, either perovskite phase or a cubic solid solution of binary oxides was formed. $DyScO_3$ first crystallized as cubic solid solution, but after annealing at 1000 °C also the perovskite phase was detected. The crystallization temperature of perovskite phases near the phase transition zone was high (800–1000 °C) but decreased rapidly when the RE^{3+} cation radius decreased and the solid solution became more favorable. $LuScO_3$ films showed a weakly crystalline structure even as deposited, before additional thermal annealing. Based on this study and several other recent publications it is obvious that several factors influence the crystallization behavior of $RESCO_3$ thin films. All $RESCO_3$ films gave smooth and clean *C–V* curves and had low leakage current densities, indicating their potential as alternative high-κ dielectric materials for MOSFETs. Highest dielectric constant was found for $DyScO_3$ (~24).

References

1 G. D. Wilk, R. M. Wallace and J. M. Anthony, *J. Appl. Phys.*, 2001, **89**, 5243–5275.
2 C. Zhao, T. Witters, B. Brijs, H. Bender, O. Richard, M. Caymax, T. Heeg, J. Schubert, V. V. Afanas'ev, A. Stesmans and D. G. Schlom, *Appl. Phys. Lett.*, 2005, **86**, 132903.
3 M. Wagner, T. Heeg, J. Schubert, C. Zhao, O. Richard, M. Caymax, V. V. Afanas'ev and S. Mantl, *Solid-State Electron.*, 2006, **50**, 58–62.
4 M. Wagner, T. Heeg, J. Schubert, St. Lenk, S. Mantl, C. Zhao, M. Caymax and S. De Gendt, *Appl. Phys. Lett.*, 2006, **88**, 172901.
5 P. Myllymäki, M. Roeckerath, M. Putkonen, S. Lenk, J. Schubert, L. Niinistö and S. Mantl, *Appl. Phys. A: Mater. Sci. Process.*, 2007, **88**, 633–637.
6 S. Van Elshocht, P. Lehnen, B. Seitzinger, A. Abrutis, C. Adelmann, B. Brijs, M. Caymax, T. Conard, S. De Gendt, A. Franquet, C. Lohe, M. Lukosius, A. Moussa, O. Richard, P. Williams, T. Witters, P. Zimmerman and M. Heyns, *J. Electrochem. Soc.*, 2006, **153**, F219–F224.
7 R. Thomas, P. Ehrhart, M. Luysberg, M. Boese, R. Waser, M. Roeckerath, E. Rije, J. Schubert, S. Van Elshocht and M. Caymax, *Appl. Phys. Lett.*, 2006, **89**, 232902.
8 R. Thomas, J. J. Saavedra-Arias, N. K. Karan, N. M. Murari, R. S. Katiyar, P. Ehrhart and R. Waser, *Solid State Commun.*, 2008, **147**, 332–335.
9 E. Durğun Özben, J. M. J. Lopes, M. Roeckerath, St. Lenk, B. Holländer, Y. Jia, D. G. Schlom, J. Schubert and S. Mantl, *Appl. Phys. Lett.*, 2008, **93**, 052902.
10 M. Roeckerath, J. M. J. Lopes, E. Durğun Özben, C. Urban, J. Schubert, S. Mantl, Y. Jia and D. G. Schlom, *Appl. Phys. Lett.*, 2010, **96**, 013513.
11 R. G. Haire and L. Eyring, in *Handbook on the Physics and Chemistry of Rare Earths*, ed. K. A. Gschneider, Jr, L. Eyring, G. R. Choppin and G. H. Lander, North-Holland Publishing, Amsterdam, 1994, vol. 18, p. 413.
12 R. P. Liferovich and R. H. Mitchell, *J. Solid State Chem.*, 2004, **177**, 2188–2197.
13 J. B. Clark, P. W. Richter and L. du Toit, *J. Solid State Chem.*, 1978, **23**, 129–134.
14 H. M. Cristen, G. E. Jellison, Jr, I. Ohkubo, S. Huang, M. E. Reeves, E. Cicerrella, J. L. Freeouf, Y. Jia and D. G. Schlom, *Appl. Phys. Lett.*, 2006, **88**, 262906.
15 T. Heeg, M. Roeckerath, J. Schubert, W. Zander, Ch. Buchal, H. Y. Chen, C. L. Jia, Y. Jia, C. Adamo and D. G. Schlom, *Appl. Phys. Lett.*, 2007, **90**, 192901.
16 P. Myllymäki, M. Nieminen, J. Niinistö, M. Putkonen, K. Kukli and L. Niinistö, *J. Mater. Chem.*, 2006, **16**, 563–569.
17 J. Päiväsaari, M. Putkonen and L. Niinistö, *Thin Solid Films*, 2005, **472**, 275–281.
18 K. J. Eisentraut and R. E. Sievers, *J. Am. Chem. Soc.*, 1965, **87**, 5254–5256.
19 *UniQuant Version 2 User Manual*, Omega Data systems, Veldhoven, Netherlands, 1994.
20 V. Sammelselg, J. Aarik, A. Aidla, A. Kasikov, E. Heikinheimo, M. Peussa and L. Niinistö, *J. Anal. At. Spectrom.*, 1999, **14**, 523–527.
21 M. Ylilammi and T. Ranta-aho, *Thin Solid Films*, 1993, **232**, 56–62.
22 M. Putkonen, T. Sajavaara, L. Niinistö and J. Keinonen, *Anal. Bioanal. Chem.*, 2005, **382**, 1791–1799.
23 S. M. George, *Chem. Rev.*, 2010, **110**, 111–131.
24 M. Nieminen, M. Putkonen and L. Niinistö, *Appl. Surf. Sci.*, 2001, **174**, 155–165.
25 M. Nieminen, T. Sajavaara, E. Rauhala, M. Putkonen and L. Niinistö, *J. Mater. Chem.*, 2001, **11**, 2340–2345.
26 M. Putkonen, T. Sajavaara, L.-S. Johansson and L. Niinistö, *Chem. Vap. Deposition*, 2001, **7**, 44–50.
27 M. Putkonen, M. Nieminen, J. Niinistö, T. Sajavaara and L. Niinistö, *Chem. Mater.*, 2001, **12**, 4701–4707.
28 B. Klingenberg and M. A. Vannice, *Chem. Mater.*, 1996, **8**, 2755–2768.
29 R. Thomas, P. Ehrhart, M. Roeckerath, S. Van Elshocht, E. Rije, M. Luysberg, M. Boese, J. Schubert, M. Caymax and R. Waser, *J. Electrochem. Soc.*, 2007, **154**, G147–G154.
30 C. Adelmann, S. Van Elshocht, A. Franquet, T. Conard, O. Richard, H. Bender, P. Lehnen and S. De Gendt, *Appl. Phys. Lett.*, 2008, **92**, 112902.
31 J. M. J. Lopes, U. Littmark, M. Roeckerath, St. Lenk, J. Schubert, S. Mantl and A. Besmehn, *J. Appl. Phys.*, 2007, **101**, 104109.
32 H. Ono and T. Katsumata, *Appl. Phys. Lett.*, 2001, **78**, 1832–1834.

